Selective pressures on C_4 photosynthesis evolution in grasses through the lens of optimality

Haoran Zhou[1], Brent R. Helliker[1] and Erol Akçay[1]

[1] Department of Biology, University of Pennsylvania, Philadelphia, PA 19104, USA

Correspondence: Haoran Zhou

Phone: 1-215-808-7042

Email: haoranzh@sas.upenn.edu

Brent R. Helliker*: helliker@sas.upenn.edu*

Erol Akçay: *eakcay@sas.upenn.edu*

Statement of authorship: HZ, BH and EA came up with the idea. HZ and EA built the model, BH put the idea in a general historical context, HZ performed the modeling work and analyzed output data. HZ wrote the first draft, BH and EA contributed substantially to revisions.

Keywords cost of C_4, evolution, optimal stomatal conductance, root-leaf allocation, water limitation, CO_2, temperature, light intensity, nitrogen allocation, dark/light reaction

Conflict of interest: None declared.

Abstract

CO_2, temperature, water availability and light intensity were potential selective pressures to propel the initial evolution and global expansion of C_4 photosynthesis in grasses. To tease apart the primary selective pressures along the evolutionary trajectory, we coupled photosynthesis and hydraulics models and optimized photosynthesis over stomatal resistance and leaf/fine-root allocation. We also examined the importance of nitrogen reallocation from the dark to the light reactions. Our results show that the higher stomatal resistance and leaf/root allocation ratio conferred by the C_4 photosynthesis led to C_4 advantage without any change in hydraulic conductance. For the initial evolution of C_4 25-32 MYA, water limitation was the primary driver, and N reallocation was necessary. Low CO_2, together with light intensity, were the primary drivers during the global radiation of C_4 5-10 MYA, during this period N reallocation would not have been strongly selected.

Introduction

Understanding the evolution of C_4 photosynthesis and the global distribution of C_3 and C_4 grasses are central questions in macro-level plant evolution and ecology. Costs and benefits of the carbon concentrating mechanism (CCM) of C_4 grasses in different climates are key to deal with these questions. Physiological models of photosynthesis focused on examining temperature and CO_2 concentration as selective pressures for C_4 evolution and expansion (Ehleringer & Monson 1993, Ehleringer et al. 1997, Collatz et al.

48 1998). They demonstrate that under warmer temperatures and low CO_2 concentration,
49 the CCM leads to less photorespiration and hence greater carbon gain in C_4, but in
50 cooler and high CO_2, the metabolic costs of the CCM and lower photorespiration leads to
51 greater carbon gain in C_3. In evolutionary terms, it is thought that as grasslands
52 expanded through the late Oligocene and early Miocene (Osborne 2008, Strömberg
53 2011), the concomitant drop in CO_2 concentration and subsequent carbon starvation
54 leading to an increase in photorespiration and the impetus for C_4 evolution in the
55 grasses. A further drop in CO_2 concentration in the late Miocene was hypothesized to
56 have led to the global-scale radiation of C_4 5-10 MYA (Edwards et al. 2010, Sage et al.
57 2012).
58
59 Recent phylogenetic evidence has, however, challenged the traditional thinking about
60 the controls on current distribution and the evolutionary impetus for C_4 in the grasses.
61 Notably, the PACMAD clade, which contains all C_4 grasses, is distributed in warm areas
62 regardless of photosynthetic pathway, whereas the BEP clade containing no C_4 grasses
63 predominates in cold areas (Edwards & Still 2008). Thus, the current global distribution
64 of C_3 and C_4 grasses might be a consequence of traits inherited from separate
65 evolutionary lineages, as opposed to differential temperature responses between C_3 and
66 C_4 photosynthesis. Additionally, water availability has emerged as a potential primary
67 selective agent in the evolution of C_4 (Edwards & Still 2008, Edwards & Smith 2010), and
68 a major contributor to current distribution of C_3 and C_4 species within a clade (Pau et al.

69 2013). C_4 photosynthesis is thought to have a higher water-use-efficiency (WUE) than C_3
70 because the CCM allows for C_4 to maintain a lower stomatal conductance for a given
71 assimilation rate (Ghannoum 2009, Taylor et al. 2014). Enhanced WUE has long been
72 suspected as the impetus for the evolution of C_4 in dicotoledenous plants (Sage 2004,
73 Edwards & Smith 2010). The potential role of water limitation in C_4 grass evolution has
74 sparked increased interest in explaining both current distributions and the anatomical
75 shifts in C_3 grasses that were prerequisites to C_4 evolution (Griffiths et al. 2012, Osborne
76 & Sack 2012, Taylor et al. 2012).
77
78 It is also likely that different selection pressures contributed to the initial evolution and
79 subsequent spread of C_4 photosynthesis. Estimates of CO_2 concentrations during the
80 initial period of C_4 evolution in the grasses 25-32 MYA, range between 350-550 ppm
81 (Cerling et al. 1997, Kürschner et al. 2008, Edwards et al. 2010, Sage et al. 2012). At the
82 low end of this range, there would likely be selection for the evolution of C_4 via the
83 carbon-starvation hypothesis, but not at the high end. On the other hand, there is a
84 general consensus that low CO_2 led to the expansion of C_4 grasses from 5-10 MYA, but
85 recent phylogenetically-based analyses show that other factors, especially water
86 availability, may play more important roles in the radiation of C_4 grasses and expansion
87 of C_4 grassland (Edwards & Smith 2010, Osborne & Freckleton 2009, Griffiths et al.
88 2012, Osborne & Sack 2012).
89

A related but largely unstudied evolutionary change during the divergence of C_4 photosynthesis from C_3 is the allocation of nutrients between the dark reactions and the light reactions. C_4 plants might allocate a greater proportion of N to light reactions than to dark reactions as compared to C_3 because of the extra ATP costs of the CCM (Tissue et al. 1995, Ghannoum et al 2010). We propose that the reallocation of N between dark and light reactions provides a further advantage for C_4 above the CCM alone, and that different environmental conditions can select for a shift in the degree of reallocation both through evolutionary time and across species in extant plants.

The physiology and phylogeographic patterns of C_4 thus suggest multiple environmental drivers might have interacted to select for C_4 evolution. Our goal in this paper is to tease apart the selective pressures that led to the evolution of C_4 photosynthesis initially, its global expansion 5-10 MYA, and its current distribution within the framework of an optimality model in which the plant makes allocation “decisions” in order to maximize its photosynthetic assimilation rate. To do this, we revisit the temperature-CO_2 crossover approach and integrate the effects of water limitation, light, optimal allocation decisions, and the interactions between these in a single model. Specifically, our model advances our understanding of C_4 evolution in four important ways. First, few modeling studies have explicitly considered multiple factors and their interactions. We incorporate water availability and light intensity as selective factors in addition to temperature and CO_2. Second, the hypothesis that C_4 photosynthesis has a higher WUE than C_3 implicitly

111 relies on an optimality argument to balance carbon gain and water loss (Medlyn et al.
112 2011, Prentice et al. 2014), yet the role of optimal stomatal conductance in mediating
113 selective pressures due to water limitation during the evolution of C_4 plants remains
114 largely unexplored (but see Way et al. 2014). Most previous models assume *a priori* that
115 C_4 grasses have lower stomatal conductance. Instead, we let both stomatal resistance
116 and leaf/fine-root allocation emerge endogenously from the model using optimality
117 arguments. Third, we include the cost of the C_4 pathway in the light reactions (2
118 additional ATP per CO_2 fixed; Hatch 1987, von Caemmerer 2000), which previous
119 models did not explicitly consider (Chen et al. 1994, Ehleringer et al. 1997, Collatz et al.
120 1992, Osborne & Sack 2012). Finally, we consider reallocation of nitrogen from the dark
121 reactions to the light reactions, which can change the tradeoffs between photosynthesis
122 and water use by C_4 grasses.
123

124 **Model construction**

125 ***Overview of the model***

126 Different modeling scenarios are used to examine the advantage of C_4 during the initial
127 origin, expansion and current distribution of C_4 photosynthesis. Initially, we assume that
128 the CCM is the only difference between C_3 and C_4. This comparison corresponds to two
129 closely related species whose other traits have not had time to diverge in response to
130 differential selection pressures. Next, we examine shifts in N allocation between light and

131 dark reactions of C_4, which may have happened in further divergence of C_3 and C_4 after

132 the CCM evolved.

133

134 The soil-plant-air water continuum was incorporated in C_3 photosynthesis models

135 (Farquhar et al. 1980) and C_4 models (von Caemmerer 2000) to examine interactions of

136 CO_2, water availability, light and temperature. We used the optimality approach of

137 Givnish (1986), where C_3 and C_4 plants optimize stomatal resistance and leaf/fine-root

138 allocation to balance carbon gain and water loss. A full model description is in

139 Supplementary Material I. The model derivation using Mathematica (Wolfram Research,

140 Inc.) and methods for numerical solutions are in Supplementary Material II.

141 ***C_3 photosynthesis model***

142 Considering the steady state of CO_2 diffusion in mesophyll cells, we get:

$$A_n = \frac{C_a - C_m}{r_s + r_m} \quad , \qquad (1)$$

144 where A_n is the net assimilation rate, C_a and C_m are the atmospheric and mesophyll CO_2

145 mixing ratios, and r_s and r_m is the stomatal and mesophyll resistance (the inverse of

146 stomatal or mesophyll conductance). A_n is computed using the FvCB model (Farquhar et

147 al. 1980) and is the minimum of two limitation states (eq. (4)): the Rubisco carboxylation

148 (dark reaction) limitation state (A_c) (eq. (2)), low CO_2 and high light intensity cause a

149 saturating supply of substrate (RuBP) for Rubisco, and reaction rate is controlled by the

150 enzyme kinetics of Rubisco; the RuBP regeneration (light reaction) limitation state(A_j)

(eq. (3)), when light intensity is low and RuBP availability limits the reaction rate. The assimilation rates are given by:

$$A_c = \frac{V_{cmax,\psi_l}(C_m - \Gamma^*)}{C_m + K_c(1 + \frac{O_m}{K_o})} - R_d \quad (2)$$

$$A_j = \frac{J_{max,\psi_l}(C_m - \Gamma^*)}{4.5C_m + 10.5\Gamma^*} - R_d \quad (3)$$

$$A_n = min(A_c, A_j) \quad , \quad (4)$$

where $V_{cmax,\psi l}$ is maximum velocity of Rubisco carboxylation (the subscript ψ_l denotes it's a function of leaf water potential), $J_{max,\ \psi l}$ is maximum rate of electron transport at a specific light intensity, R_d is the mitochondrial respiration rate in the daytime and Γ^* is CO_2 compensation point of photosynthesis. O_m is O_2 concentration in the mesophyll cell, which is assumed equal to atmospheric O_2. K_c and K_o are the Michaelis-Menten constants of Rubisco for CO_2 and O_2.

C_4 photosynthesis model

For the C_4 pathway, we consider the steady state mixing ratio of CO_2 in both mesophyll (C_m) and bundle sheath cells (C_{bs}), which gives us two equations:

$$A_n = V_p - g_{bs}(C_{bs} - C_m) \quad (5)$$

$$A_n = \frac{(C_a - C_m)}{(r_s + r_m)} + R_{dm} \quad , \quad (6)$$

where g_{bs} is the bundle sheath conductance, V_p is the PEP carboxylation rate, ($g_{bs}(C_{bs}-C_m)$) represents bundle sheath leakage from bundle sheath cells back to mesophyll and R_{dm} are the daytime mitochondrial respiration rate in mesophyll cells.

171 The PEP carboxylation rate V_p is limited by either PEPc carboxylation (eq. (7)), which

172 follows a Michaelis-Menten type or PEP regeneration (eq. (8))

$$V_p = \frac{V_{pmax,\psi_l} C_m}{C_m + K_p} \quad (7)$$

$$V_p = x J_{max}/3 \quad , \quad (8)$$

175 where $V_{pmax,\psi l}$ is maximal PEPc carboxylation rate, K_p is the Michaelis-Menten coefficient

176 of PEPc for CO_2 and x is the fraction of total electron transport could be used for the PEP

177 regeneration, which represents the cost of the CCM. The denominator 3 in eq. (8) arises

178 due to the fact that regeneration of 1 molecule of PEP needs 2 additional ATP, which is 3

179 additional electrons transported. Thus, equations (8) and (10) incorporate the cost of C_4

180 pathway. A_c and A_j of C_4 are given by

$$A_c = \frac{V_{cmax,\psi_l}(C_{bs} - \Gamma^*)}{C_{bs} + K_c(1 + \frac{O_{bs}}{K_o})} - R_d \quad (9)$$

$$A_j = \frac{(1-x) J_{max,\psi_l}(C_{bs} - \Gamma^*)}{4.5 C_{bs} + 10.5\Gamma^*} - R_d \quad (10)$$

183 which is obtained by substituting C_m in eq. (2) and (3) with C_{bs}.

184 Based on equations (7), (8), (9) and (10), A_n of C_4 is limited by four states as follows:

$$A_n = min(A_{cc}, A_{cj}, A_{jc}, A_{jj}) \quad . \quad (11)$$

186 Here, A_{cc} is RuBP carboxylation and PEPc carboxylation limited rate; A_{cj} is RuBP

187 carboxylation and PEP regeneration limited rate; A_{cj} is PEP carboxylation and RuBP

188 regeneration limited rate; and A_{jj} is limited by PEP regeneration and RuBP regeneration

189 limited rate.

190

191 ***Hydraulic system***

Eq. (12) describes the soil-plant-air continuum (Givnish 1986). At equilibrium, the rate of water loss through transpiration equals the rate of water absorption by the roots:

$$\frac{EfN}{\rho} = k(1-f)N(\psi_l - \psi_s) \quad , \qquad (12)$$

where Ψ_s is soil water potential, k is the effective root hydraulic conductivity, N is the total biomass of fine root and leaves, ρ is the leaf mass density (gcm^{-2}) and E is the transpiration rate per leaf area. E could be written as δ/r_s, where δ is the water partial pressure deficit between saturated leaf surface and the atmosphere. Thus, leaf water potential (Ψ_l) is a function of r_s and leaf/fine-root allocation (f, defined as investment into leaves/total investment in leaves and fine root)).

$$\psi_l = \psi_s - \frac{f\delta}{\rho k r_s(1-f)} \qquad (13)$$

Inhibition of photosynthesis by water stress

Reduced leaf water potential inhibits photosynthesis (Tezara et al. 1999, Lawlor & Cornic 2002, Tang 2002). We model this cost of transpiration as Weibull-type vulnerability curves relating leaf Ψ_l and photosynthetic parameters (Vico & Porporato 2008):

$$V_{cmax,\psi_l} = V_{cmax} e^{-(\frac{-\psi_l}{d_v})^{b_v}} \qquad (14)$$

$$J_{max,\psi_l} = J_{max} e^{-(\frac{-\psi_l}{d_j})^{b_j}} \qquad (15)$$

$$V_{pmax,\psi_l} = V_{pmax} e^{-(\frac{-\psi_l}{d_p})^{b_p}} \quad , \qquad (16)$$

where b and d are curve fitting parameters. Since Ψ_l is a function of r_s and f, all those parameters are functions of r_s and f.

213

214 ***Optimal stomatal resistance and optimal allocation of energy between leaves and fine***

215 ***roots***

216 We assume that the plant adjusts the r_s and f to optimize the total carbon gain by

217 $A_{total} = fNA_n/\rho$, (16)

218 where ρ is the leaf mass density (g cm^{-2}). As a simplifying assumption, we assume N and

219 ρ are fixed (similar to Givnish, 1986). Effectively, we consider the optimization problem

220 faced by the plant in a given instance during its growth, where its size (of which N is a

221 proxy) can be regarded as a constant. Clearly, during plant growth, the assimilate will be

222 turned into plant biomass, but the instantaneous optimization problem will still yield the

223 optimal growth path, as it maximized the growth rate at any given time. Finally, we regard

224 ρ as a species-specific trait that changes at a slower time-scale than r_s and f. The first

225 order optimality conditions for r_s and f are given by (Givnish 1986):

226 $$\frac{\partial(fA_n)}{\partial r_s} = f\frac{\partial A_n}{\partial r_s} = 0 \quad (17)$$

227 $$\frac{\partial(fA_n)}{\partial f} = A_n + f\frac{\partial(A_n)}{\partial f} = 0 \quad . \quad (18)$$

228 We checked the second order derivative to ensure that the numerical solutions to the

229 first order conditions were maxima.

230

231 ***Allocation of nitrogen***

232 We examine how nitrogen allocation between RuBP carboxylation and RuBP
233 regeneration in C_4 grasses affect competitive advantage over C_3 grasses. Despite great
234 variation in V_{cmax} and J_{max} based on the total leaf nitrogen content within C_3 plants,
235 Wullschleger (1993) found a mean of J_{max}/V_{cmax} =2.1 across 109 C_3 species, which we
236 use as a baseline for C_3 and C_4 pathways in analyzing the initial evolution of C_4. Then,
237 we used J_{max}/V_{cmax} =4.5 for C_4 (Vico & Porporato 2008, Osborne & Sack 2012) to
238 analyze the role that nitrogen reallocation played in the evolutionary trajectory of C_4
239 plants. In determining the values of J_{max} and V_{cmax}, we used a simplified stoichiometry:
240 we consider the total of J_{max} and V_{cmax} as a constant to hold nitrogen concentration
241 constant (Vico & Porporato 2008, Osborne & Sack 2012). Two assumptions are
242 underlying this simplified stoichiometry: (1) investing one molecule of nitrogen to the dark
243 reactions will increase of V_{cmax} equal to the increase of J_{max} by investing one molecule of
244 nitrogen to the light reactions; (2) nitrogen allocation to photorespiration and to the CCM
245 balanced each other.
246
247 ***Modeling scenarios***
248 We modeled the photosynthesis rates of C_3 and C_4 under temperature range from 10 °C
249 to 40 °C with an interval of 5 °C, under CO_2 mixing ratios ranging from 200 ppm to 600
250 ppm with an interval of 50 ppm, under different water conditions (VPD=0.001, 1, 2, 3,
251 4kPa corresponding to soil water potential (Ψ_S) =0, -0.5, -1, -1.5, -2 MPa) and under
252 different light intensities (1400, 1000, 600, 200, 100 μmol photons $m^{-2}s^{-1}$). We consider

253 VPD=0.001 kPa and Ψ_S =0 MPa as saturated water condition and light intensity of 1400

254 µmol photons m^{-2} s^{-1} as an average saturated light intensity of a day.

255

256 ## Results

257 ### C_3/C_4 crossover temperatures and environmental variations

258 We numerically solved for assimilation-based crossover temperatures, defined as the

259 temperature at which assimilation by the C_4 pathway starts exceeding that by the C_3,

260 across the full range of CO_2, evaporative conditions, and soil-water availability, all under

261 saturated light. In the first scenario (Fig. 1a), we assume the same allocation of N to light

262 and dark reactions in the C_3 and C_4 plants (specifically, J_{max}/V_{cmax}=2.1 for both). Across

263 all CO_2 concentrations, the crossover temperature decreases as water limitation

264 increased. Under the most extreme water-stressed conditions (VPD = 4 kPa, Ψ_S =-2

265 MPa), the crossover temperatures are all below 5°C, even under a CO_2 of 600 ppm, and

266 C_4 plants have an advantage at all temperatures.

267

268 In our second scenario, we assume a reallocation between RuBP regeneration and

269 RuBP carboxylation processes in C_4 by changing the J_{max}/V_{cmax} ratio to 4.5 while keeping

270 it at 2.1 in C_3 (Fig. 1b). The crossover temperatures are lower than the first scenario

271 under saturated water conditions through to VPD = 3 kPa and Ψ_S = -1.5 MPa, suggesting

272 that reallocation increases the advantage of C_4 in those conditions. Under low CO_2 and

273 low water availability (e.g. CO_2=300 ppm, VPD = 3 kPa and Ψ_S = -1.5 MPa or all CO_2

274 concentrations with VPD = 4 kPa and Ψ_S = -2 MPa), however, crossover temperatures
275 are comparatively higher than those of J_{max}/V_{cmax}=2.1, showing that reallocation
276 decreases the C_4 advantage under water limitation and low CO_2.
277
278 Under saturated soil water availability, low VPD, and identical light- and dark-reaction
279 allocation of C_3 and C_4, crossover temperatures decrease along with increasing light
280 intensity (Fig. 1c). An increase in light intensity provides a larger relative benefit for C_4 at
281 low CO_2, because C_3 photosynthesis is CO_2 limited and C_4 is light limited. The crossover
282 temperatures under all light intensities reach 40 ^{o}C, when CO_2 is above 350 ppm. With
283 the change of J_{max}/V_{cmax} (Fig. 1d), crossover temperatures decrease at every light
284 intensity. The high-light result in Fig. 1d predicts a C_3/C_4 crossover temperature of 23°C
285 under 380 ppm, similar to previous models that did not explicitly account for water stress
286 (Ehleringer et al. 1997, Collatz et al 1998).
287
288 **Stomatal resistance and leaf root allocation**
289 Under all scenarios and both for C_3 and C_4 plants, optimal r_s first decreases as
290 temperature increases, and then increases and it increases monotonically with
291 increasing CO_2 (Fig. 2 a, c, e). Throughout the range of water availability we considered,
292 optimal r_s is higher for C_4 than C_3 at temperature ranging from 10 to 40 ^{o}C and CO_2
293 ranging from 200 to 600 ppm. The optimal f has a similar relationship of an inverse
294 U-shape curve along with temperature. Increasing CO_2 results in an increase of leaf

295 allocation (Fig. 2 b, d, f). Optimal *f* for C_3 is always higher than that for C_4 under different
296 water availability and CO_2. *f* decreases as intensity of water limitation increase. Results
297 are the same for C_4 with a J_{max}/V_{cmax} of 4.5 (not shown).
298

299 **RuBP carboxylation versus regeneration limitations**

300 The C_3 pathway transitions from being CO_2 limited under low temperatures to light
301 limited under high temperatures. The jumps in r_s and *f* in Fig. 2 correspond to the
302 transition from RuBP carboxylation limited assimilation (A_c) to RuBP regeneration limited
303 assimilation (A_j) of C_3, and the transition from RuBP carboxylation and PEP regeneration
304 limited (A_{jc}) to RuBP regeneration and PEP regeneration limited assimilation (A_{jj}) of C_4.
305 The transition temperature decreases as CO_2 increases. In the Fig. S1, A_c, A_j, A_{cc}, A_{cj}, A_{jc}
306 and A_{jj} are plotted together under several environmental scenarios, using both
307 J_{max}/V_{cmax}=2.1 and 4.5 for C_4. With J_{max}/V_{cmax}=2.1, C_4 is light limited in all the
308 environmental conditions. With J_{max}/V_{cmax}=4.5, C_4 starts to be limited by CO_2 under low
309 temperatures and to be limited by light under high temperatures.
310

311 **Quantifying differences in C-assimilation rate**

312 While crossover temperatures allow for a clear diagnostic of comparative assimilation,
313 they do not demonstrate the degree of difference. To this end, we calculated the net
314 assimilation rate difference between C_4 and C_3, ΔA_n (net assimilation of C_4 minus that of
315 C_3), under different conditions (Fig. 3 and 4). Under a CO_2 concentration of 200 ppm and

316 saturated light, ΔA_n is higher under moister conditions than water-limited conditions (Fig.
317 3a). In contrast, under higher CO_2 concentrations (400 and 600 ppm), C_4 has an
318 advantage only in serious water limited conditions, which leave a relatively small scope
319 for C_4 to evolve (areas where $\Delta A_n > 0$ in Fig. 3c, e). This result is due to the fact that C_3
320 photosynthesis has a greater proportional increase in assimilation from 200 to 400 and
321 600 ppm CO_2. However, the change of J_{max}/V_{cmax} increases both the ΔA_n and space for
322 C_4 advantage (Fig. 3 b, d, f). Similar with water availability, at 200 ppm, ΔA_n is highest
323 under saturated light, and decreases as light intensity decreases (Fig. 4a). ΔA_n is
324 relatively constant and negative across all light intensities at 400 ppm CO_2 (Fig. 4c). The
325 change of J_{max}/V_{cmax} also increases the ΔA_n and space for C_4 advantage under different
326 light intensities (Fig. 4 b, d).
327
328 Finally, we calculate the photosynthesis rates of the two pathways under conditions often
329 encountered in today's grasslands to look at the effect of nitrogen reallocation between
330 RuBP carboxylation and regeneration: CO_2 =400 ppm, saturated light with three water
331 conditions (Fig. 5). With J_{max}/V_{cmax} =2.1 for both C_3 and C_4, the C_4 assimilation rate is
332 rarely higher than C_3, which indicates C_4 does not have an obvious advantage under
333 current CO_2 from saturated water conditions through to VPD = 2 kPa and Ψ_S = -1 MPa in
334 current grassland because of the cost of the CCM. However, with J_{max}/V_{cmax} =4.5 for C_4,
335 C_4 does have an advantage over C_3 at temperatures above 25 ^{o}C.
336

Discussion

Changes in the climate that occurred towards the end of the Oligocene about 30 MYA led to a drier Earth; the consequent increase in wildfires and seasonal droughts forced the forests then covering the earth to give way to entirely new biomes: the grasslands and savannas (Strömberg 2011). The open and drier habitats populated by these ancestral grasses would have had higher temperatures due to greater incident radiation and an uncoupling from the turbulent mixing of air above the grass canopy, which exacerbate physiological challenges by increasing water loss from the leaf to the atmosphere. Furthermore, higher temperatures and a decrease in atmospheric CO_2 would have increased photorespiration in these ancestral C_3 grasses. Therefore, grasses encountered several environmental changes during the evolution of C_4: CO_2, temperature, water availability, increasing irradiance, and the reallocation of nutrients as the CCM evolved. Previous work has considered most of these factors separately, meaning potential interactions between them remain unexplored. We took a comprehensive approach to elucidate the multi-faceted selective pressures on early C_4 grassland evolution, the expansion of C_4 5-10 MYA and current distribution in an optimization framework.

Selective pressures and interactions among CO_2, temperature, water availability and light

357 We find that water limitation is the primary selective pressure for the evolution of C_4
358 grasses when CO_2 is above 400 ppm, suggesting that the environmental pressures for
359 C_4 evolution were in place during the early expansion of grass-dominant biomes. During
360 the early origins of C_4 (25-30 MYA), estimates of CO_2 concentrations are typically above
361 400 ppm (Cerling et al. 1997, Kürschner et al. 2008, Edwards & Smith 2010). Under
362 saturated water conditions, the predicted crossover temperature at 400 ppm is above 40
363 °C because the benefits of the CCM are outweighed by the costs, indicating there is little
364 room for C_4 to evolve. However, as water becomes more limited, the predicted crossover
365 temperature ranges between 20 °C to 30 °C, while the C_4 advantage (ΔA_n) becomes
366 increasingly larger due to the higher WUE conferred by the C_4 CCM. Our work therefore
367 adds to the growing body of evidence that the primary selective factor for C_4 grass
368 evolution was enhanced carbon gain under water limited conditions, in accordance with
369 phylogenetic evidence (Edwards et al. 2010, Pau et al. 2013), and what has generally
370 been believed to be the selective force behind the evolution of C_4 in dicotyledonous
371 plants (Sage 2004).
372
373 In a recent physiological model, Osborne and Sack (2012) also suggest a hydrological
374 underpinning to the competitive success of C_4 grasses, but found a much smaller
375 environmental window for C_4 evolution than we did. At 400 ppm and Ψ_S = -1 MPa, they
376 showed that C_4 hydraulic conductance must be twice that of C_3 grasses for C_4 grasses to
377 achieve greater carbon uptake. In contrast, we find a clear C_4 advantage under these—

378 and even drier— conditions by allowing for optimal solutions of r_s and f to maximize A_n,
379 while keeping plant hydraulic conductance equal across C_3 and C_4. Our results do not
380 contradict the idea that larger bundle sheaths and smaller IVD— which were
381 prerequisites for C_4 evolution (Griffiths et al. 2012, Christin et al. 2013) — led to greater
382 hydraulic conductance among C_3 grass progenitors (Griffiths et al. 2012), but they do
383 suggest that greater hydraulic conductance is not necessary to give C_4 plants an
384 advantage once the CCM evolved.
385
386 As CO_2 decreased through the Miocene, C_4 grasses saw a large-scale global expansion
387 5-10 MYA. Our results suggest that at this time, the main selective force for C_4 evolution
388 shifted from water limitation to low CO_2 and, to a lesser extent, light intensity. Low CO_2
389 provides a clear advantage for C_4 under all water availability and light intensity regimes.
390 Under low CO_2, the greatest ΔA_n occurs in relatively saturated-water and
391 mild-water-limited conditions, opposite what is seen under high CO_2, and suggesting
392 water limitation is not as effective of a selective pressure under low CO_2. Our results are
393 consistent with previous studies showing that low CO_2 (200-300 ppm) is a selective
394 pressure for C_4 species (e.g. Ehleringer et al. 1997).
395
396 Since light intensity is not an important selective force under high CO_2, it seems likely
397 that C_4 grasses could not dominate open grasslands, except in very arid areas, while
398 CO_2 was still high. However, when CO_2 decreased to ~300 ppm and below (Cerling et al.

399 1997, Kürschner et al. 2008, Edwards & Smith 2010), high light intensity provided an
400 enhanced advantage for C_4 (crossover temperature decreases, and ΔA_n increases).
401 These findings give mechanistic support to the idea that between the initial evolutionary
402 events leading to the emergence of C_4 grasses and the large-scale expansion 5-10
403 MYA, C_4 radiation idled in small pockets of selective favorability as CO_2 concentrations
404 declined through the Miocene (Christin et al. 2008, Sage 2004). As CO_2 declined, the
405 high light levels inherent to grassland systems gave C_4 photosynthesis an increasing
406 selective advantage, leading to broader geographic and evolutionary radiation.
407
408 **The role of nitrogen allocation in C_4 evolution and expansion**
409 We assumed that during the early evolution of the CCM, both C_3 and C_4 plants had a
410 similar balance of nitrogen across the light and dark reactions. Subsequent to the
411 evolution of CCM, selection could favor the reallocation of nitrogen from dark to light
412 reactions (increasing J_{max}/V_{cmax}). In general, CCMs allow for less investment in
413 nitrogen-rich Rubisco (Ku et al. 1979, Christin & Osborne 2014), and the nitrogen not
414 used for Rubisco could be either reinvested in light harvesting machinery, or simply not
415 used at all. Increasing J_{max}/V_{cmax} almost always increases the photosynthesis rate of C_4
416 grasses (Fig. S2), and therefore could lead to a competitive advantage over C_3 grasses
417 as well as C_4 grasses that do not reallocate. Assuming there is little cost or no genetic
418 constraints for reallocation, the selection pressure to reallocate would have been
419 strongest when CO_2 was high, i.e., during the initial evolutionary events in the

420 Oligocene/Miocene, when the CCM alone does not give C_4 a large advantage (low ΔA_n
421 in Fig. 3c). When CO_2 was low during the C_4 radiation 5-10 MYA, however, the CCM
422 alone would give C_4 an advantage and reallocation would not change the competitive
423 balance between C_3 and C_4. As CO_2 remained low through to the Pleistocene, selection
424 for nitrogen reallocation to the light reactions would lessen further, especially during the
425 CO_2 minima of the Pleistocene glacial periods (~ 180 ppm). In this context, an interesting
426 question is whether the high CO_2 of the last 150 years is selecting for increased
427 J_{max}/V_{cmax} today.
428
429 Modeling studies have assumed a high J_{max}/V_{cmax} for C_4 photosynthesis, while the few
430 empirical estimates of J_{max}/V_{cmax}, in C_4 plants paint a more variable picture for extant C_4
431 species. C_4 photosynthesis models assumed J_{max}/V_{cmax} to be around 4.5 with the same
432 sum of J_{max} and V_{cmax} for C_3 and C_4 (Vico & Porporato 2008, using a fit from Collatz et al.
433 1992, Osborne & Sack 2012). C_4 species have lower Rubisco content and higher
434 chlorophyll and thylakoid content, giving evidence of reallocation in extant C_4 species
435 (Tissue et al. 1995, Ghannoum et al. 2010, Vogan & Sage 2012). In contrast,
436 empirically-based estimates of C_4 J_{max}/V_{cmax} range from less than 2 to above 6, with a
437 mean of about 4 (Domingues et al. 2007, Massad et al. 2007, Grant et al. 2007,
438 Kathilankal et al. 2011, Ye et al. 2013, Ge et al. 2014), which is lower than model
439 assumptions, but still higher than the mean J_{max}/V_{cmax} estimates for C_3 plants of 2.1
440 (Wullschleger 1993). Our results suggest that nitrogen availability and environmental

441 factors (water, CO2, light) have likely affected natural variation in J_{max}/V_{cmax} observed in

442 extant species, as well as through evolutionary time.

443

444 Conclusion

445 Our results show that by optimizing carbon gain over water loss, we can tease apart the

446 selective factors for C_4 evolution in the grasses in both the relatively high CO_2 conditions

447 of the late Oligocene/Early Miocene and the late Miocene expansion. At any CO_2

448 concentration above 400 ppm, water limitation was the primary selective factor for C_4

449 evolution, and even at 600 ppm there is room for C_4 evolution under the driest

450 conditions. Furthermore, we find that the CCM alone leads to enough of a reduction in

451 water use that there would have been little selection for increased hydraulic conductance

452 within C_4 grasses. Below 400 ppm, CO_2 and to a lesser extent light, become the

453 dominant selective pressures, leading to gains in net C_4 carbon assimilation that greatly

454 exceeded those under higher CO_2. We therefore have a plausible physiological

455 explanation for why C_4 grasses could have evolved hand-in-hand with the grassland

456 biome, even though they did not achieve ecological dominance for many millions of

457 years until CO_2 concentrations dropped.

458

459 C_4 photosynthesis first evolved in the grasses 25 – 32 MYA, and many subsequent and

460 independent evolutionary origins occurred well into the Pleistocene 2.8 MYA. Each

461 evolutionary origin potentially represents both different selective pressures and

taxonomic (genetic) constraints as climate and CO_2 changed. Taking the Chloridoideae as an example, our model suggests that initial evolution of C_4 photosynthesis 25 – 32 MYA (Christin et al. 2008) was driven by aridity, acting to decrease stomatal conductance that increased photorespiration in C_3 progenitors initially, and led to higher water use efficiency upon the evolution of the CCM. Also at this point, there would have been strong selection for reallocation of nitrogen from the dark reactions to the light reactions. The large radiation of C_4 within the Chloridoideae that occurred 5 – 10 MYA was likely driven by low CO_2 and high light. There would have been much less selective pressure to reallocate N at this point, but such a reorganization was likely already in place within the clade. In contrast, for the lineages that first evolved C_4 in the late Miocene (e.g. *Stipagrostis*, *Eriachne*, *Neurachne*), CO_2 would have been the primary impetus for C_4 evolution, but for these lineages there would have been little impetus to reallocate nitrogen until the dawn of the industrial revolution. In many ways this examination of nitrogen allocation is speculative, but it nonetheless illustrates how we can use comprehensive physiological models to tease apart variation in C_4 physiology along the evolutionary trajectory. Furthermore, by selecting extant species within select lineages, nitrogen stoichiometry can be examined empirically, ultimately providing an integrative view of the selection pressures that led to the extant physiology and distribution of C_4 plants.

Acknowledgements

We are grateful for support from the University of Pennsylvania as well as undying assistance from Qing Zhang, Jemma Lloyd-Helliker and Ebru Erdem-Akçay.

References

1. von Caemmerer, S. (2000). Biochemical models of photosynthesis. In Techniques in Plant Sciences. CSIRO Publishing, Colingwood, Australia, pp 91–122.

2. Cerling, T.E., Harris, J.M., MacFadden, B.J., Leakey, M.G., Quade, J., Eisenmann, V. & Ehleringer, J.R. (1997). Global vegetation change through the Miocene/Pliocene boundary. Nature, 389, 153-158.

3. Chen, D.-X., Coughenour, M.B., Knapp, A.K. & Owensby, C.E. (1994). Mathematical simulation of C_4 grass photosynthesis in ambient and elevated CO_2. Ecol. Model., 73, 63–80.

4. Christin P.A., Besnard G., Samaritani E., Duvall M.R., Hodkinson T.R., Savolainen V. & Salamin N. (2008). Oligocene CO2 decline promoted C_4 photosynthesis in grasses. Curr. Biol., 18, 37–43.

5. Christin, P.A., Osborne, C.P., Chatelet, D.S., Columbus, J.T., Besnard, G., Hodkinson, T.R., Garrison, L.M., Vorontsova, M.S. & Edwards, E.J. (2013). Anatomical enablers and the evolution of C_4 photosynthesis in grasses. Proc. Natl. Acad. Sci. USA, 110, 1381-1386.

6. Christin, P.A. & Osborne, C.P. (2014). Tansley Review. The evolutionary ecology of C_4 photosynthesis. New Phytol., 204, 765-781.

7. Collatz, G.J., Berry, J.A. & Clark, J.S. (1998). Effects of climate and atmospheric CO_2 partial pressure on the global distribution of C_4 grasses: present, past, and future. Oecologia, 114, 441-454.

8. Collatz, G.J., Ball, J.T., Grivet, C. &Berry, J.A. (1992). Coupled photosynthesis-stomatal conductance model for leaves of C_4 plants. Aust. J. Plant Physiol., 19, 519-538.

9. Domingues, T.F., Martinelli, L.A. & Ehleringer, J.R. (2007). Ecophysiological traits of plant functional groups in forest and pasture ecosystems from eastern Amazônia, Brazil. Plant Ecol., 193, 101-112.

10. Edwards, E.J., Osborne, C.P., Strömberg, C.A.E., Smith, S.A. & C4 Grasses Consortium. (2010). The Origins of C_4 Grasslands: Integrating Evolutionary and Ecosystem Science. Science, 328, 587-591.

11. Edwards, E.J. & Smith, S.A. (2010). Phylogenetic analyses reveal the shady history of C_4 grasses. Proc. Natl. Acad. Sci. USA, 107, 2532-2537.

12. Edwards, E.J. & Still, C.J. (2008). Climate, phylogeny and the ecological distribution of C_4 grasses. Ecol. Lett., 11, 266-276.

13. Ehleringer, J.R. & Monson, R.K. (1993). Evolutionary and ecological aspects of photosynthesis pathway variation. Annu. Rev. Ecol. Syst., 24, 411-439.

14. Ehleringer, J.R., Cerling, T.E. & Helliker, B.R. (1997). C_4 photosynthesis, atomospheric CO_2, and climate. Oecologia, 112, 285-299.

15. Farquhar, G.D., Von Caemmerer, S. & Berry, J.A. (1980). A biochemical model of photosynthetic carbon dioxide assimilation in leaves of 3-carbon pathway species. Planta, 149, 78–90.

16. Ge, Z.M., Zhang, L.Q., Yuan, L. & Zhang, C. (2014). Effects of salinity on temperature-dependent photosynthetic parameters of a native C3 and a non-native C4 marsh grass in the Yangtze Estuary, China. Photosynthetica, 52, 484–492.

17. Ghannoum, O. (2009). C_4 photosynthesis and water stress. Ann. Bot., 103, 635–644.

18. Ghannoum, O., Evans, J.R. & von Caemmerer, S. (2010). Nitrogen and water use efficiency of C_4 plants. In: *C_4 photosynthesis and related CO_2 concentrating mechanisms* (eds. Raghavendra, A.S. & Sage, R.F.). Springer Science, The Netherlands, Dordrecht, pp. 129–146.

19. Givnish, T.J. (1986). Optimal stomatal conductance, allocation of energy between leaves and roots, and the marginal cost of transpiration. In: *On the Economy of Plant Form and Function* (ed. Givnish TJ). Cambridge University Press, Cambridge, pp. 171–213.

20. Grant, R.F. & Flanagan, L.B. (2007). Modeling stomatal and nonstomatal effects of water deficits on CO_2 fixation in a semiarid grassland. J. Geophys. Res.,112, G03011, doi:10.1029/2006JG000302.

21. Griffiths, H., Weller, G., Toy, L. & Dennis, R.J. (2012). You're so vein: bundle sheath physiology, phylogeny and evolution in C_3 and C_4 plants. Plant Cell Environ., 36, 249–261.

22. Hatch, M.D. (1987). C_4 photosynthesis: a unique blend of modified biochemistry, anatomy and ultrastructure. Biochim. Biophys. Acta, 895, 81-106.

23. Kathilankal, J.C., Mozdzer, T.J., Fuentes, J.D., McGlathery, K.J., D'Odorico, P. & Zieman, J.C. (2011). Physiological responses of Spartina alterniflora to varying environmental conditions in Virginia marshes. Hydrobiologia, 669, 167-181.

24. Ku, M.S.B., Schmitt, M.R. & Edwards, G.E. (1979). Quantitative determination of RuBP carboxylase-orygenase protein in leaves of several C_3 and C_4 plants. J. Exp. Bot., 114, 89–98.

25. Kürschner, W.M., Kvacek, Z. & Dilcher, D.L. (2008). The impact of Miocene atmospheric carbon dioxide fluctuations on climate and the evolution of terrestrial ecosystems. Proc. Natl. Acad. Sci. U S A, 105, 449-453.

26. Lawlor, D.W. & Cornic, G. (2002). Photosynthetic carbon assimilation and associated metabolism in relation to water deficits in higher plants. Plant Cell Environ., 25, 275–294.

27. Massad, R.S., Tuzet, A. & Bethenod, O. (2007). The effect of temperature on C_4-type leaf photosynthesis parameters. Plant Cell Environ., 30, 1191-1204.

28. Medlyn, B.E., Duursma, R.A., Eamus, D., Ellsworth, D.S., Prentice, I.C., Barton, C.V.M., Crous, K.Y., De Angelis, P., Freeman, M. & Wingate, L. (2011). Reconciling the optimal and empirical approaches to modelling stomatal conductance. Glob. Chang Biol., 17, 2134-2144.

29. Osborne, C. P. (2008). Atmosphere, ecology and evolution: what drove the Miocene expansion of C_4 grasslands? J. Ecol., 96, 35-45.

30. Osborne, C.P. & Freckleton, R.P. (2009). Ecological selection pressures for C_4 photosynthesis in the grasses. Proc. Biol. Sci., 276, 1753-1760.

31. Osborne, C.P. & Sack, L. (2012). Evolution of C_4 plants: a new hypothesis for an interaction of CO_2 and water relations mediated by plant hydraulics. Philos. Trans. R. Soc. Lond. B. Biol. Sci., 367, 583-600.

32. Pau, S., Edwards, E.J. & Still, C.J. (2013). Improving our understanding of environmental controls on the distribution of C_3 and C_4 grasses. Glob. Chang Biol., 19, 184-196.

33. Prentice, I. C., Dong, N., Gleason, S.M., Maire, V. & Wright, I.J. (2014). Balancing the costs of carbon gain and water transport: testing a new theoretical framework for plant functional ecology. Ecol. Lett. 17, 82-91.

34. Sage, R.F. (2004). The evolution of C4 photosynthesis. New Phytol., 161, 341-370.

35. Sage, R.F., Sage, T.L. & Kocacinar F. (2012). Photorespiration and the evolution of C_4 photosynthesis. Annu. Rev. Plant Biol., 63, 19-47.

36. Strömberg, C.A.E. (2011). Evolution of grasses and grassland system. Annu. Rev. Earth Planet Sci., 39, 517-544.

37. Tang, A.C. (2002). Photosynthetic oxygen evolution at low water potential in leaf discs lacking an epidermis. Ann. of Bot., 89, 861-870.

38. Taylor, S.H., Franks, P.J., Hulme, S.P., Spriggs, E., Christin, P.A., Edwards, E.J., Woodward, F.I. & Osborne, C.P. (2012). Photosynthetic pathway and ecological adaptation explain stomatal trait diversity amongst grasses. New Phytol., 193, 387-396.

39. Taylor, S.H., Ripley, B.S., Martin, T., De-Wet, L.-A., Woodward, F.I. & Osborne, C.P. (2014). Physiological advantages of C_4 grasses in the field: a comparative experiment demonstrating the importance of drought. Glob. Change Biol., 20, 1922-2003.

40. Tezara, W., Mitchell, V.J., Driscoll, S.D. & Lawlor, D.W. (1999). Water stress inhibits plant photosynthesis by decreasing coupling factor and ATP. Nature, 401, 914-917.

41. Tissue, D.T., Griffin., K.L., Thomas, R.B. & Strain, B.R. (1995). Effects of low and elevated CO_2 on C_3 and C_4 annuals. II. Photosynthesis and leaf biochemistry. Oecologia, 101, 21-28.

42. Vico, G. & Porporato, A. (2008). Modelling C_3 and C_4 photosynthesis under water-stressed conditions. Plant and Soil, 313, 187-203.

43. Vogan, P.J. & Sage R.F. (2012). Effects of low atmospheric CO_2 and elevated temperature during growth on the gas exchange responses of C_3, C_3–C_4 intermediate,

and C_4 species from three evolutionary lineages of C_4 photosynthesis. Oecologia, 169, 341-352.

44. Way, D.A., Katul, G.G., Manzoni, S. & Vico, G. (2014). Increasing water use efficiency along the C_3 to C_4 evolutionary pathway: a stomatal optimization perspective. J. Exp. Bot., 65, 3683-3693.

45. Wullschleger, S.D. (1993). Biochemical limitations to carbon assimilation in C_3 plants - A retrospective analysis of the A/C_i curves from 109 species. J. Exp. Bot., 44, 907-920.

46. Ye Z., Suggett, D.J., Robakowski, P., Kang, H. (2013). A mechanistic model for the photosynthesis-light response based on the photosynthetic electron transport of photosystem II in C_3 and C_4 species. New Phytol., 199: 110–120.

686 Figure Legends

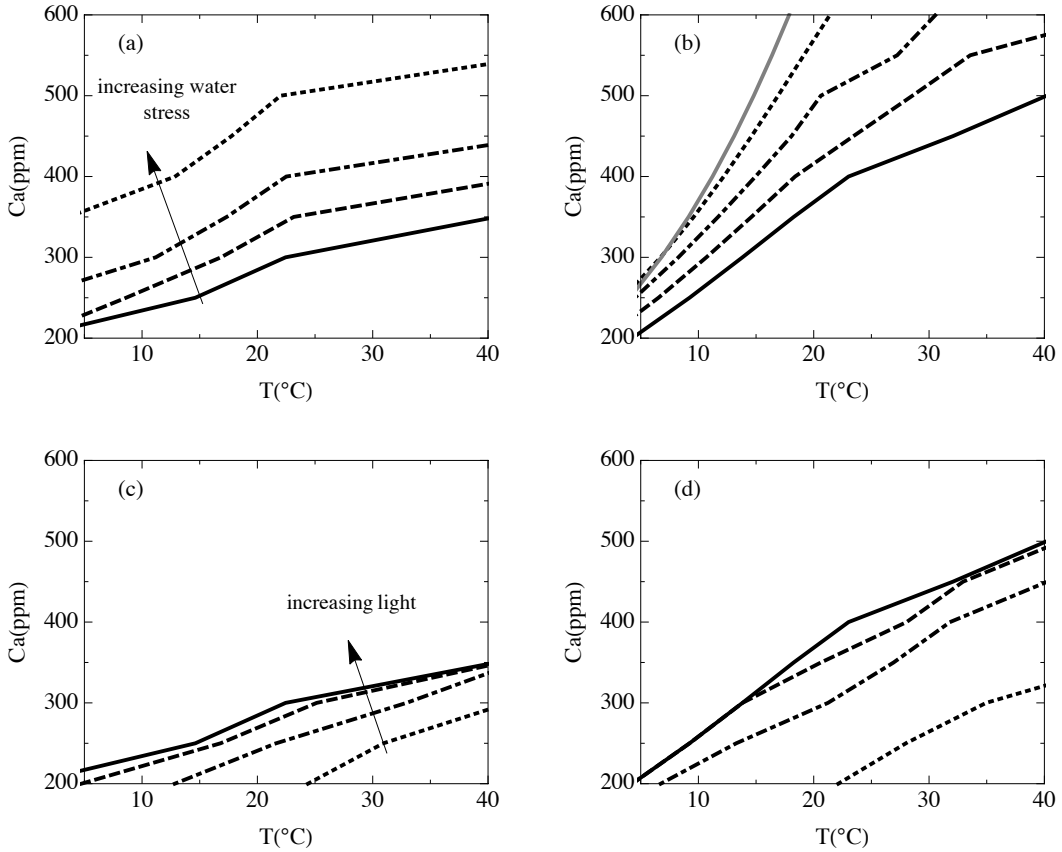

687

688 Fig. 1. (a) Crossover temperatures of photosynthesis for C_3 and C_4 with the change of

689 CO_2 concentration under different water conditions. Light intensity was 1400 μmol

690 photons $m^{-2}s^{-1}$ and J_{max}/V_{cmax}=2.1 for C_3 and C_4; (b) same as (a) except J_{max}/V_{cmax}=2.1

691 for C_3 and J_{max}/V_{cmax}=4.5 for C_4. Solid black line: VPD=0.15kPa, Ψ_S=0 MPa; dashed

692 black line: VPD=1kPa, Ψ_S=-0.5 MPa; dot-dashed black line: VPD=2kPa, Ψ_S=-1 MPa;

693 dotted black line: VPD=3 kPa, Ψ_S=-1.5 MPa; solid gray line: VPD=4 kPa, Ψ_S=-2 MPa. (c)

694 Crossover temperatures with the change of CO_2 concentration under different light

695 intensities under saturated water condition (VPD=0.15kPa, Ψ_S=0 MPa). J_{max}/V_{cmax}=2.1

696 for C_3 and C_4, (d) same as (c) except J_{max}/V_{cmax}=2.1 for C_3 and J_{max}/V_{cmax}=4.5 for C_4.

697 Solid black line: 1400 µmol photons $m^{-2}s^{-1}$; dashed black line: 1000 µmol photons $m^{-2}s^{-1}$;

698 dot-dashed black line: 600 µmol photons $m^{-2}s^{-1}$; dotted black line: 200 µmol photons

699 $m^{-2}s^{-1}$.

700

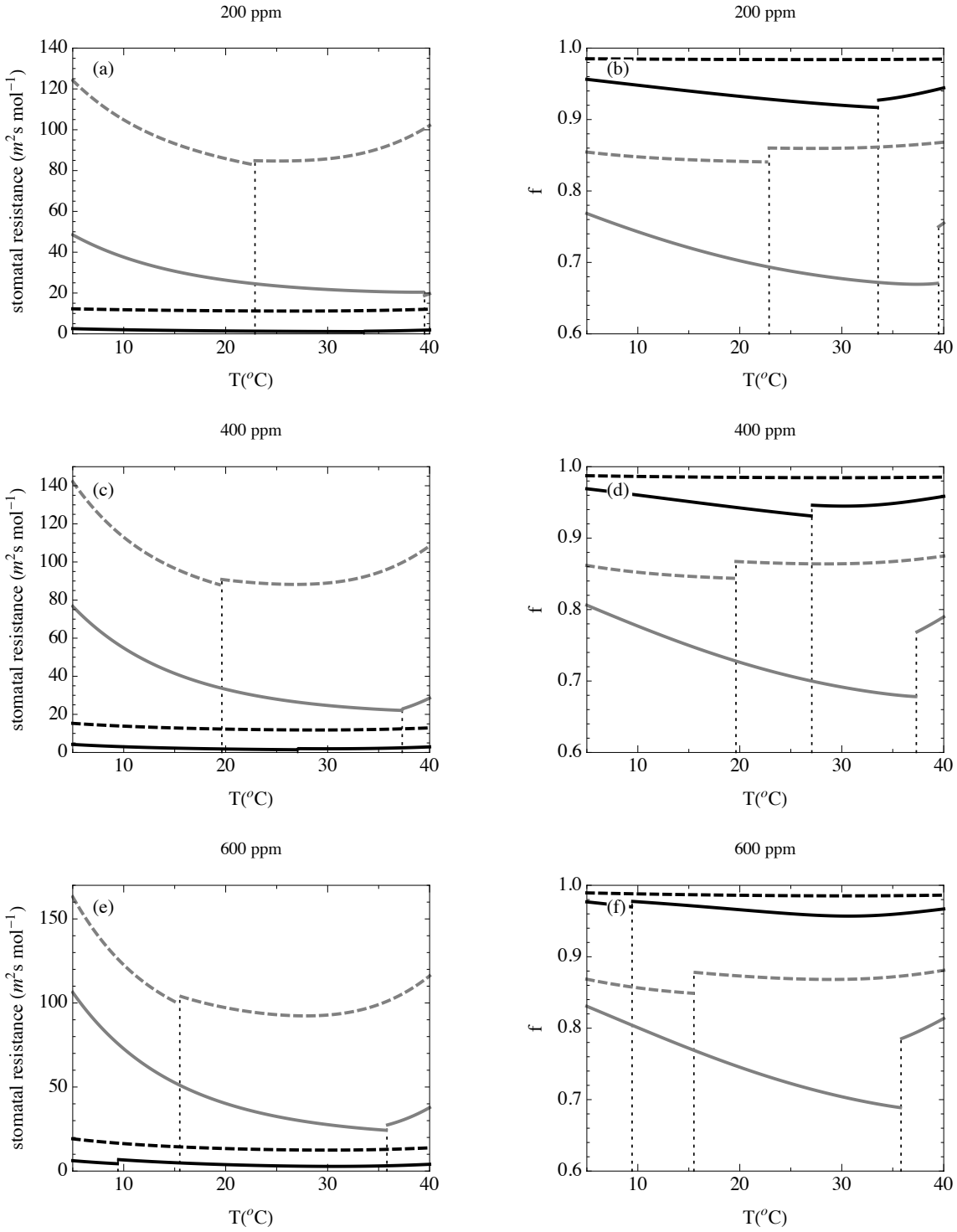

Fig. 2. Stomatal resistance (r_s) and leaf allocation (f) as a function of temperature, with J_{max}/V_{cmax}=2.1 for both C_3 and C_4 with saturated light under different CO_2 (200 ppm, 400

704 ppm and 600 ppm) and different water conditions. Solid black line: C_3 with

705 VPD=0.15kPa, Ψ_S=0 MPa; dashed black line: C_4 with VPD=0.15kPa, Ψ_S=0; solid grey

706 line: C_3 with VPD=4 kPa, Ψ_S=-2 MPa; dashed grey line: C_4 with VPD=4 kPa, Ψ_S=-2 MPa.

707 Vertical lines indicate transition from RuBP carboxylation limited condition to RuBP

708 regeneration limited condition for C_3; for C_4, all the transition temperatures<5 °C.

709

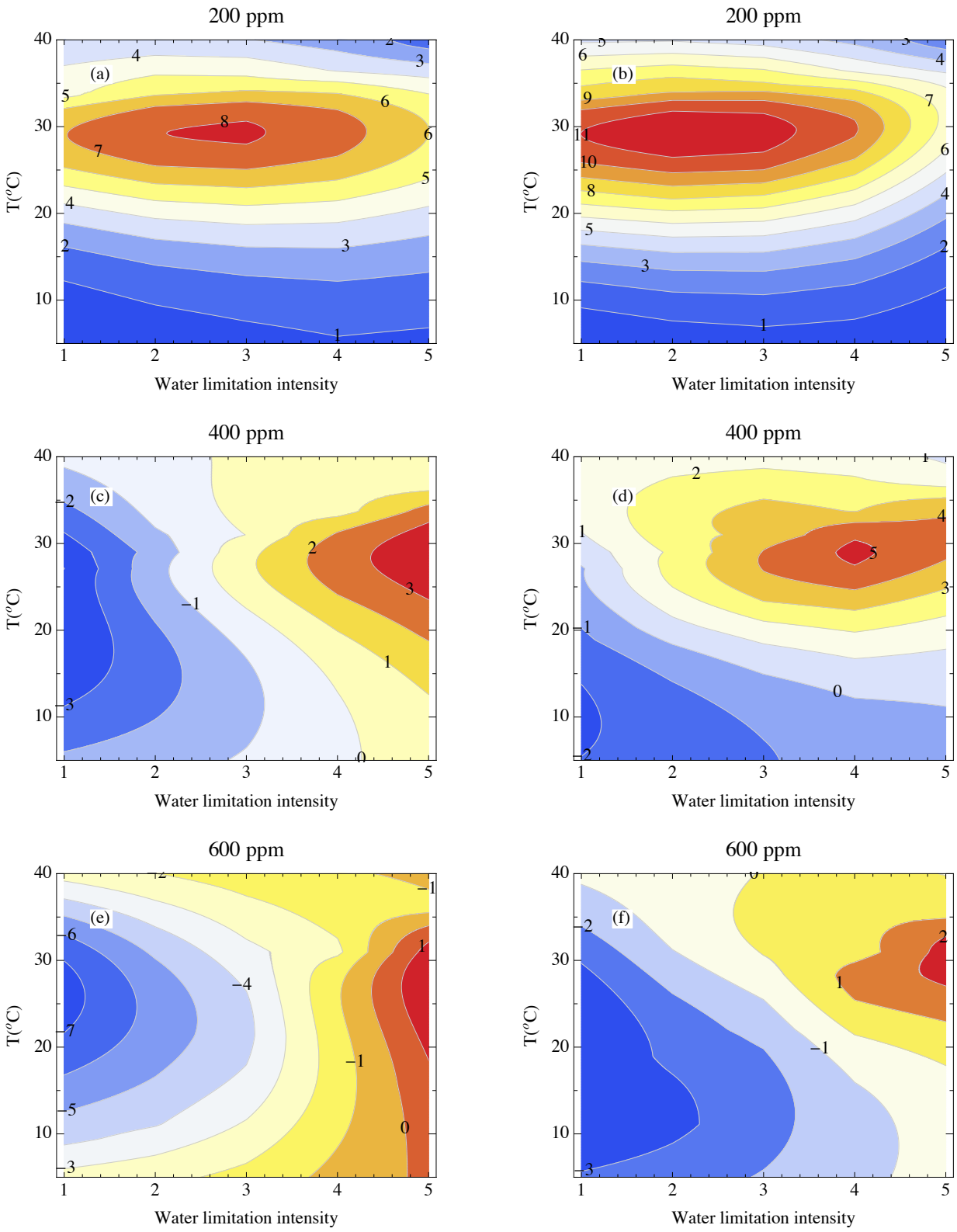

Fig. 3. Contour plot of modeled assimilation difference between C_4 and C_3 ($A_n(C_4)$-$A_n(C_3)$) with J_{max}/V_{cmax}=2.1 for C_3 and C_4 under various CO_2 (200 ppm, 400 ppm

713 and 600 ppm) and saturated light intensity (1400 µmol photons $m^{-2}s^{-1}$), various water

714 conditions (a, c, e) and with J_{max}/V_{cmax}=2.1 for C_3 and J_{max}/V_{cmax}=4.5 for C_4 (b, d, f).

715 Water limitation intensity 1, 2, 3, 4, 5 refers to VPD=0.15kPa, Ψ_S=0 MPa; 1.5 kPa,

716 -0.5MPa; 2kPa, -1 MPa; 3kPa, -1.5 MPa; 4kPa, -2 MPa.

717

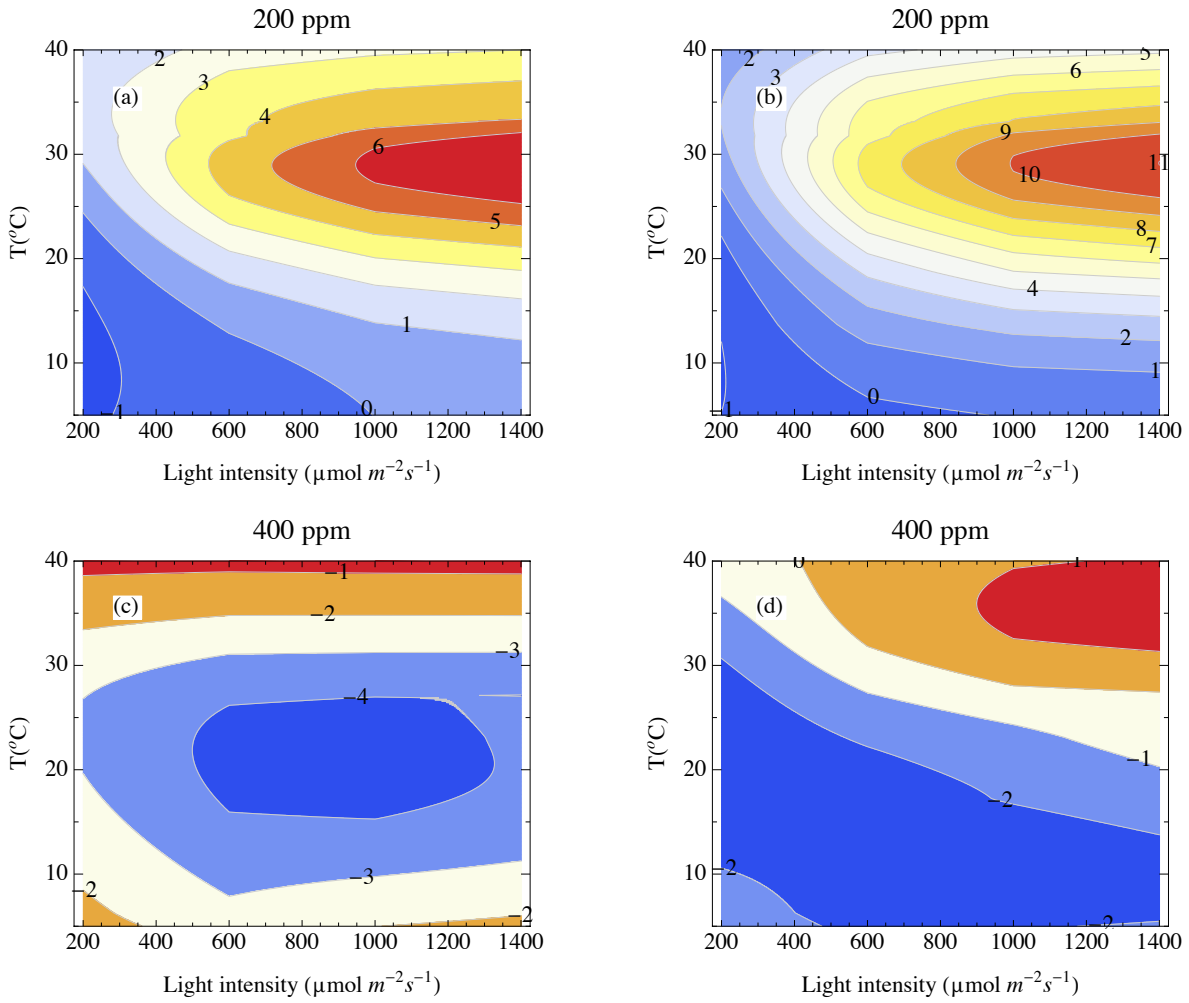

718

719 Fig. 4. Contour plot of modeled assimilation difference between C_4 and C_3

720 ($A_n(C_4)$-$A_n(C_3)$) with J_{max}/V_{cmax}=2.1 for C_3 and C_4 under various CO_2 (200 ppm, 400 ppm)

721 and different light intensities (from 200 to 1400 µmol photons $m^{-2}s^{-1}$) with saturated water

condition (VPD=0.15kPa, Ψ_S=0 MPa) (a, c) and with J_{max}/V_{cmax}=2.1 for C_3 and J_{max}/V_{cmax}=4.5 for C_4 (b, d).

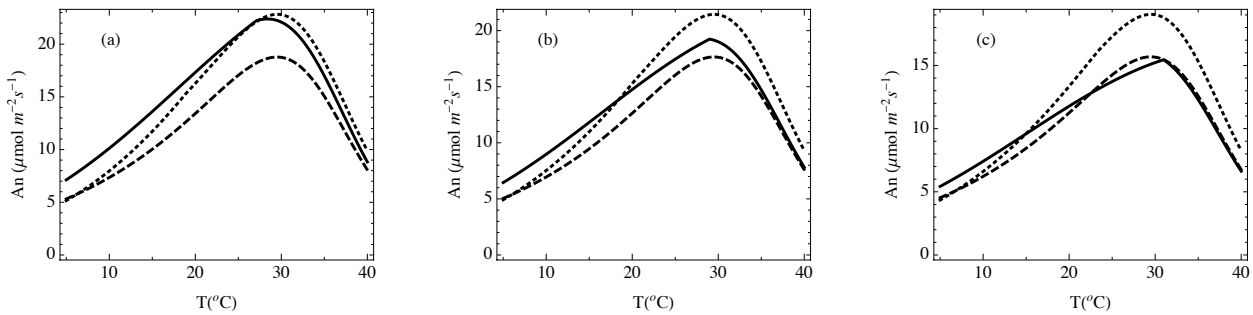

Fig. 5. Assimilation rates of C_3 with J_{max}/V_{cmax}=2.1 (solid black line), C4 with J_{max}/V_{cmax}=2.1 (dashed black line) and C_4 with J_{max}/V_{cmax}=4.5 (dotted black line) under light intensity of 1400 µmol photons $m^{-2}s^{-1}$, CO_2 of 400 ppm and different water limitated conditions. (a) saturated soils; (b) VPD=1kPa and Ψ_S=-0.5 MPa; (c) VPD=2kPa and Ψ_S=-1 MPa.